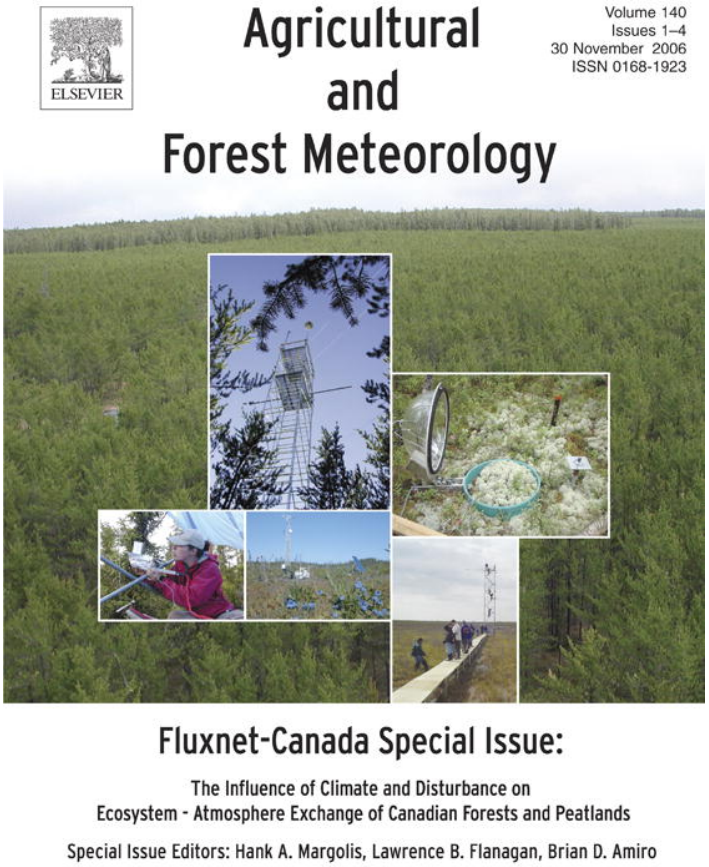

Available online at www.sciencedirect.com
ScienceDirect
Agricultural and Forest Meteorology 140 (2006) 257–268
AGRICULTURAL AND FOREST METEOROLOGY
www.elsevier.com/locate/agrformet

Leaf area index measurements at Fluxnet-Canada forest sites

Jing M. Chen [a,*], Ajit Govind [a], Oliver Sonnentag [a], Yongqin Zhang [a], Alan Barr [b], Brian Amiro [c]

[a] *Department of Geography, University of Toronto, 100 St. George Street, Toronto, Ontario, Canada M5S 3G3*
[b] *Meteorological Service of Canada, Environment Canada, Saskatoon, Saskatchewan, Canada S7N 3H5*
[c] *Department of Soil Science, University of Manitoba, Winnipeg, Manitoba, Canada R3T 2N2*

Received 16 November 2005; accepted 22 March 2006

Abstract

Leaf area index (LAI) measurements made at 17 forest sites of the Fluxnet Canada Research Network are reported here. In addition to LAI, we also report other major structural parameters including the effective LAI, element clumping index, needle-to-shoot area ratio, and woody-to-total area ratio. Values of the fraction of photosynthetically active radiation (FPAR) absorbed by green leaves in these stands at noon of 15 August are also provided, and a procedure is suggested for using the effective LAI for estimating FPAR at various times of the day and year. Labour-intensive laboratory measurements of the needle-to-shoot area ratio were made for five conifer sites. For each site, 45 shoot samples were measured at three heights from three trees. LAI-2000, TRAC and digital hemispherical photography (DHP) were used in the field, and good agreements between these techniques were obtained. In particular, the low cost DHP technique agreed within 21% of LAI-2000 in terms of effective LAI measurements and 12% of TRAC in terms of element clumping index measurements, suggesting a possibility of using DHP alone for indirect LAI measurements. However, LAI-2000 and TRAC are still found to be more reliable than DHP because of some remaining technical issues with DHP. We confirm the correct method for determining the photographic exposure proposed in previous studies and suggest optimum zenith angle ranges in photograph processing to estimate the effective LAI and the clumping index.

Keywords: LAI; FPAR; TRAC; LAI-2000; Digital hemispherical photography; Clumping; Multiple scattering

1. Introduction

The leaf area index, defined as one half the total green leaf area per unit ground surface area (Chen and Black, 1992a; see also review by Jonckheere et al., 2004), is a basic and indispensable parameter for interpreting carbon, water and energy fluxes measured at tower sites. It is also of interest to modelers who attempt to upscale these tower fluxes to regions based on biospheric data. The Fluxnet Canada Research Network (FCRN) stresses, in its network design, the importance of acquiring accurate and consistent LAI measurements across the network by forming a special task team to visit all forest sites in the network. The LAI values of all FCRN main forests sites and some satellite sites are reported here.

Through previous works, various LAI indirect measurement techniques have been tested, and theories behind these techniques are becoming mature (Jonckheere et al., 2004; Weiss et al., 2004). These techniques are shown to be comparable with labour-intensive direct (destructive) measurements (Chen et al., 1997; Gower et al., 1999). However, indirect measurements of LAI still

* Corresponding author. Tel.: +1 416 978 7085.
E-mail addresses: chenj@geog.utoronto.ca (J.M. Chen), Alan.barr@ec.gc.ca (A. Barr), Brian_Amiro@umanitoba.cpa (B. Amiro).

0168-1923/$ – see front matter © 2006 Elsevier B.V. All rights reserved.
doi:10.1016/j.agrformet.2006.08.005

face challenges in quantifying foliage clumping at various scales, and in particular, clumping of needles in shoots in conifer stands is one of the main sources of LAI measurement error (Chen et al., 1997). Based on previous film-based hemispherical works (Brown, 1962; Anderson, 1964; Olsson et al., 1982; Chan et al., 1986; Rich, 1990; Chen et al., 1991; Baret et al., 1993; Whitford et al., 1995), digital hemispherical photography (DHP) techniques are becoming increasingly popular (Englund et al., 2000; Frazer et al., 2001; Wagner, 2001; Walter et al., 2003; Leblanc et al., 2005; Zhang et al., 2005) as a digital camera system costs less than other instruments and contain much detailed canopy structural information. The gap size analysis theory of Chen and Cihlar (1995) has been applied to hemispherical photographs (Walter et al., 2003; Leblanc et al., 2005) and multi-band canopy images (Kucharik et al., 1999) to address the issue of foliage clumping. There seems to be a potential that a digital camera system can substitute all current LAI instruments including LAI-2000 (Li-Cor, Nebraska, USA) and TRAC (Third Wave Engineering, Ottawa, Canada) for measurements in forest stands. In addition to reporting LAI values and their components in forest sites in Fluxnet Canada, the purpose of this present study is also to investigate several technical issues in LAI measurements including: (i) fast and reliable laboratory measurements of the needle-to-shoot area ratio to quantify within-shoot clumping, and (ii) the reliability of DHP gap fraction analysis to obtain the effective LAI and the reliability of DHP gap size analysis to obtain the clumping information.

2. LAI measurement theory

Through previous theoretical development and validation (Chen, 1996a; Chen et al., 1997), the following governing equation is used for determining LAI (denoted as L):

$$L = \frac{(1-\alpha)L_e\gamma_E}{\Omega_E} \tag{1}$$

where α is the woody-to-total leaf area ratio, L_e the effective LAI, γ_E the needle-to-shoot area ratio, and Ω_E is the element clumping index. The effective LAI can be accurately measured using the LAI-2000 instrument, or less accurately with a hemispherical photography technique (Zhang et al., 2005), based on the Miller (1967) theory (Chen, 1996a):

$$L_e = 2\int_0^{\pi/2} \ln\left[\frac{1}{P(\theta)}\right]\cos\theta\sin\theta\,d\theta \tag{2}$$

where $P(\theta)$ is the measured canopy gap fraction at zenith angle θ, which is the best when averaged over the entire azimuthal angle range. Accurate measurement of L_e requires hemispherical $P(\theta)$ data, and both LAI-2000 and hemispherical photography can provide the data through sensing the diffuse radiation from the sky over the hemisphere. While there are issues of the accuracy of hemispherical photography techniques associated with exposure and processing (Chen et al., 1991; Wagner, 2001; Zhang et al., 2005), LAI-2000 can provide reliable estimates of L_e, although the multiple scattering effect can cause a considerable underestimation of L_e and should be corrected (Chen, 1996b).

The remaining major challenge in optical LAI measurements lies in getting the other parameters in Eq. (1). The determination of α should theoretically require destructive sampling because green and non-green materials in conifer canopies are not easily separated by optical means, although Kucharik et al. (1997) developed an instrument for this purpose. Even though non-green materials can be differentiated from green materials from an upward-looking camera in multiple spectral bands, the probability of their overlapping would incur considerable uncertainty (Kucharik et al., 1999). In this study, this parameter in conifer stands was not measured, but we rely on estimates based on forest age and hemispherical photographs where the amount of tree trunks is clearly visible. In a broadleaf stand, it was estimated through LAI-2000 measurements before the growing season using the methodology of Barr et al. (2004).

Foliage clumping (Nilson, 1971) is separated into two scales: within-shoot clumping and beyond-shoot clumping (Chen and Cihlar, 1995). This separation is necessary because optical instruments are generally incapable of measuring gaps between needles within a shoot. This level of foliage clumping was recognized and estimated in various ways by Oker-Blom (1986), Gower and Norman (1990), Stenberg et al. (1994), Fassnacht et al. (1994), etc. Based on a theoretical development by Chen (1996a), this clumping is quantified using the needle-to-shoot area ratio (γ_E) as follows:

$$\gamma_E = \frac{A_n}{A_s} \tag{3}$$

where A_n is half the total needle area (including all sides) in a shoot, and A_s is the half the shoot area defined as

$$A_s = \frac{1}{\pi}\int_0^{2\pi} d\phi \int_0^{\pi/2} A_p(\theta,\phi)\cos\theta\,d\theta \tag{4}$$

where ϕ is the azimuthal angle difference between the direction of light and the main axis of the shoot, θ the zenith angle, and $A_p(\theta,\phi)$ is the projected area of the shoot. If the shoot is spherical, the projected area is the same in all directions, and A_s would be twice A_p, i.e. the hemispherical area is twice the projected area (disk). Procedures in using Eq. (4) in practice are given in Section 3.5.

Beyond-shoot clumping (Ω_E) is quantified using the element clumping index and measured directly in the field using either TRAC or DHP based on a canopy gap size distribution theory (Chen and Cihlar, 1995; Leblanc et al., 2005). This clumping includes the effect of canopy structures larger than shoots, including tree crowns, whorls, branches, etc. It is determined using the following equation (Chen and Cihlar, 1995; Leblanc, 2002):

$$\Omega_E(\theta) = \frac{\ln[F_m(0,\theta)]}{\ln[F_{mr}(0,\theta)]} \frac{[1 - F_{mr}(0,\theta)]}{[1 - F_m(0,\theta)]} \quad (5)$$

where $F_m(0,\theta)$ is the total canopy gap fraction at zenith angle θ, i.e. the accumulated gap fraction from the largest to smallest gaps; and $F_{mr}(0,\theta)$ is the total canopy gap fraction after removing large gaps resulting from the non-random foliage element distribution due to canopy structures such as tree crowns and branches.

3. Sites and experimental methods

3.1. Site description and LAI transects

Most FCRN sites that are measured in this study are described in Coursolle et al. (2006), and the description of the eastern white pine sites near the Turkey Lake is found in Peichl and Arain (2006). Therefore, only the main attributes of these sites are provided in Table 1. Also shown in Table 1 are LAI transects established at each flux tower site. At a site, LAI measurements were made along one or two transects of length ranging from 60 to 400 m depending on the homogeneity and size of a

Table 1
Site description and location and LAI transects

Site	Code	Age (2005)	Latitude, longitude	Overstorey	Transect directions (from north)	Transect lengths (m)
Intermediate Douglas Fir, Campbell River, B.C.	IDF	54	49.905, 125.366	*Pseudotsuga menziesii*	46°, 226°	200, 200
1988 Douglas Fir, Campbell River, B.C.	DF88	14	49.519, 124.902	*P. menziesii*	46°, 226°	150, 200
Old Mixed Wood, Timmins, Ontario	OMW	74	48.217, 82.156	*Picea mariana*	270°	400
Eastern Old Black Spruce, Chibougamo, Quebec	EOBS	100	49.692, 74.342	*P. mariana*	270°, 90°	400, 300
1980 Balsam Fir Charlie Lake, NB	BF80	25	46.472, 67.100	*Abies balsamea*	270°	200
Intermediate Balsam Fir Nashwaak Lake, NB	IBF	38	46.474, 67.098	*A. balsamea*	270°	300
Young Balsam Fir Nashwaak Lake, NB	YBF	32	46.477, 67.077	*A. balsamea*	325°	300
1942 White Pine Plantation, Turkey Lake, Ontario	WPP39	66	42.710, 80.357	*Pinus strobus*	180°	200
1970 White Pine Plantation Turkey Lake, Ontario	WPP74	31	42.709, 80.348	*P. strobus*	180°	200
1985 White Pine Plantation, Turkey Lake, Ontario	WPP89	16	42.773, 80.459	*P. strobus*	180°	200
1977 Fire Candle Lake, Sask.	F77	28	54.485, 105.817	*Pinus banksiana*	0°	100
1998 Fire Candle Lake, Sask.	F98	7	53.917, 106.078	*P. banksiana*	90°	100
Old Aspen, Prince Albert, Sask.	OA	84	53.629, 106.200	*Populus tremuloides*	225°, 135°	300, 60
Southern Old Black Spruce Candle Lake, Sask.	SOBS	123	53.987, 105.117	*P. mariana*	135°, 67°	100, 60
Southern Old Jack Pine Candle Lake, Sask.	SOJP	88	53.916, 104.690	*P. banksiana*	135°, 67°	200, 60
1975 Harvested Jack Pine, Candle Lake, Sask.	HJP75	30	53.875, 104.045	*P. banksiana*	135°, 325°	150, 150
1994 Harvested Jack Pine, Candle Lake, Sask.	HJP94	11	53.908, 104.690	*P. banksiana*	325°	100

More descriptions are in Coursolle et al. (2006).

site. At the mixed hardwood site at Timmins, for example, where the stand is extensive and variable because of the species mixture, the transect was 400 m long, while at the eastern white pine (*Pinus stobus* L.) sites near Turkey Lake, where the stand size is limited but uniform, only 200 m transects were measured. At satellite sites, transects are correspondingly short. The transects generally ran from the flux tower to the prevailing wind direction in order to characterize the portion of the canopy that influences most the measured energy, water and carbon fluxes. At the Douglas-fir (*Pseudotsuga menziesii* (Mirb.) Franco) sites on the Vancouver Island, the transects ran in two directions from the tower: southwest (226° from north) and northeast (46° from north) corresponding to the daytime sea-breeze direction and nighttime Katabatic flow direction, respectively. The directions of transects given in Table 1 are the compass baring subtracted by the magnetic north (varying between sites), so they are in geographic coordinates.

3.2. LAI measurement protocol

We followed the LAI measurement protocol of Chen et al. (2002) to estimate all needed parameters in Eq. (1):

(1) To measure the effective LAI (L_e) at all sites, using LAI-2000 as the main instrument. With new development in measurement techniques, a DHP technique can be used as an alternative when recommended procedures are followed (Zhang et al., 2005).
(2) To measure the element clumping index (Ω_E) at all sites, using TRAC as the main instrument. The alternative DHP technique can also be used for this purpose, but generally with less accuracy (Leblanc et al., 2005).
(3) To measure the needle-to-shoot area ratio (γ_E) where possible. Otherwise suggested default values for various forest types can be used (Chen, 1996a). This current study suggests more values.
(4) To measure the woody-to-total area ratio (α) where possible. Otherwise they can be estimated based on forest types and age according to previous experimental results (Chen, 1996a; Kucharik et al., 1998).

In the present study, we focus on the following issues in the protocol: (i) using DHP for clumping estimation through applying Chen and Cihlar (1995) gap size analysis method, and (ii) reducing errors in LAI estimation by carrying out a large amount of labour-intensive measurements of the needle-to-shoot area ratio. While further research is still needed to measure the woody-to-total area ratio non-destructively, we only use the best estimates on this parameter for the final LAI estimation using Eq. (1). Although this measurement protocol is developed based on our experience with boreal forests, it would be applicable to other ecosystems. We encourage other flux networks to carry out LAI measurements using consistent techniques and protocols so that flux data can be effectively compared across sites and networks.

3.3. LAI-2000 and TRAC measurements

Along the transect(s) at each site, forestry marker flags were inserted to the forest floor every 10 m. Generally, two LAI-2000 units were used each time, one mounted on the top of the tower in a continuous logging mode and one used inside the stand at each flag. As different units were used each time, they were synchronized and calibrated following recommended procedures in the LAI-2000 manual. The measurements were made either in the evening when the sun is below 75° from the zenith or under an overcast sky. A 90° view cap was used on both units to block any remaining direct light and to avoid the influence of the operator on the sensor. The operator always stood between the sensor and the sun.

The TRAC was walked on the same transect on clear days, and at each 10 m flag, a distance mark was registered in the data stream by pressing a button. In dense stands where the TRAC sensor did not fully expose to the sun, reference measurements for the direct light above the canopy was made in a large opening or outside the stand. In addition to measuring the element clumping index, TRAC also produces the effective LAI and the LAI after using additional inputs of the needle-to-shoot area ratio and woody-to-total area ratio. In heterogeneous stands, the effective LAI from TRAC could be significantly different from that from LAI-2000 as TRAC measures it only along the sun's direction while LAI-2000 provides the average for the hemisphere. We therefore used the effective LAI from LAI-2000 in our final LAI calculation.

Although LAI-2000 provides the average effective LAI for a much larger angular domain than does TRAC, it can suffer from a large error due to multiple scattering of light in the canopy. This is because the instrument assumes that leaves are black in blue wavelengths (400–490 nm) used for canopy gap fraction estimation, but in reality leaves have considerable blue scattering albedos. This multiple scattering effect on LAI retrieval is most

significant at the largest zenith angles at which the gap fraction is smallest. A useful way to investigate this multiple scattering effect is to ignore rings 4 and 5 of LAI-2000 data using the available C2000 software, corresponding to the zenith angle ranges from 45° to 60° and 60° to 74°, respectively, to see the impact of these rings on the calculated LAI. The caveat of this approach is the assumption of a spherical leaf angle distribution, i.e. the extinction coefficient being a constant. This assumption may not be valid for conifer canopies, which often have vertical tree crowns and horizontal branches. We will assess the effect of this assumption on LAI estimation in Section 4.

3.4. Hemispherical photograph acquisition and processing

We took the opportunity of network-wide LAI measurements to test the utility of the digital hemispherical photography (DHP) technique for LAI measurements, based on the recent work by Leblanc et al. (2005). DHP data were acquired at most sites using a Nikon CoolPix 4500 digital camera with a Nikon FC-E8 fisheye lens. In order to test the accuracy of DHP for both the effective LAI and the element clumping index estimation, the exposure of the photographs followed a strict procedure, based on the recommendation of Zhang et al. (2005). Briefly, the correct exposure for a photograph taken inside a stand was determined universally to be two stops of overexposure relative to the sky reference exposure, i.e. the automatic exposure of the sky determined outside the stand. Since the reference exposure often changed considerably, especially near sunset, between the start and end of measurements along a transect, L_e at a location near the middle of the transect was taken as the weighted mean of L_e values calculated separately with two photographs taken at two exposures referenced to the sky exposure at the beginning and end of the measurements, respectively. We normally took three to five photographs of different exposures at a flag position.

Fisheye photographs were processed with the DHP software to derive the effective LAI (Leblanc et al., 2005). Based on two threshold values, the software identifies pixels of pure sky, pure plant, and mixture of these two, and an unmixing method is used to estimate the gap fraction within mixed pixels (Leblanc et al., 2005). A circular photograph was divided into concentric 15 rings spanning the zenith angle range from 0° to 75°. To avoid problems of missing small gaps in DHP at large zenith angles, the effective LAI was calculated using the ring corresponding to zenith angle range of 55–60°, following the recommendation of Leblanc et al. (2005). The clumping index was derived through the combined use of the DHP and TRAC softwares. In DHP, a string of digital numbers along a concentric circle on the photograph, corresponding to a zenith angle, was extracted from each photograph and imported to TRAC software, where this string was treated as a TRAC measurement along a transect and converted it to canopy gaps of various sizes, from which the element clumping index was estimated. The DHP software allows this data string extraction at 1° intervals over the entire zenith angle range from 0° to 75°, and the clumping variation with zenith angle was investigated by Leblanc et al. (2005). Generally, the index increases with zenith angle by about 20% from zenith to 75°. This increase is caused by both structural and optical reasons. Structurally, large gaps disappear at large zenith angles, making the canopy appear less clumped (higher clumping index). Optically, the measured gap size distribution may be distorted at large zenith angles because the image resolution (normally 1704 × 2272 pixels) is still not high enough to resolve all small gaps, making the foliage element size considerably larger than the shoot size in conifer stands. In this study, therefore, we computed the element clumping index from DHP within the zenith angle range 40–45°, a compromise of the suggested angle of 57.5° (Leblanc et al., 2005) and measurement accuracy.

3.5. Needle-to-shoot area ratio measurement

In each forest stand, 45 shoot samples were taken from three trees: one dominant (D), one co-dominant (M) and one suppressed (S), at three heights: top (T), middle (M) and bottom (L), forming nine classes containing five shoot samples each: DT, DM, DL, MT, MM, ML, MS, ST, SM, and SL (e.g., DT means top height of a dominant tree). They were taken from trees either via a canopy access tower or a crane lift. These samples were kept in electrical coolers at a temperature slightly above 0 °C and analyzed within a week in laboratory. A system, consisting of a digital camera (Toshiba PDR-4300) mounted on a firm copy stand (Regent Instruments Inc., Canada), a light table (Kaiser Prolite 5000, Germany), and a Windows-based personal computer with an image analysis software, was used to measure the projected shoot areas. The volume displacement method described in Chen et al. (1997) was used to measure the needle area in a shoot. As no empirical coefficients were available in Chen et al. (1997) for converting the volume to the surface area for needles with elliptical cross sections (Douglas-fir, balsam fir [*Abies balsamea* (L.) Mill.]) and of bifurcated

cylinder shapes (eastern white pine), we develop additional empirical equations according to needle thickness (a) to width (b) ratio:

$$A_n = f\sqrt{Vnl} \tag{7}$$

where f is a shape factor for elliptical and bifurcated cylinders separately:

$$f_{\text{elliptical}} = 0.5\sqrt{\pi h \times \left(1 + \frac{1}{h}\right)}, \quad h = \frac{a}{b} \tag{8}$$

and

$$f_{\text{b-cylinder}} = \sqrt{\frac{n}{\pi}} + \sqrt{\frac{\pi}{n}} \tag{9}$$

where n is the number of bifurcations. For eastern white pine, $n = 5$.

The calculation of the half the total shoot area needed for estimating the needle-to-shoot area ratio is based on Eq. (4). As many shoot samples were analyzed, we took the approach of Chen (1996a) to measure the projected shoot area at only three camera incidence angles: 0°, 45° and 90° relative to the shoot main axis at one azimuth angle of 0°, i.e. obtaining $A_p(0°, 0°)$, $A_p(45°, 0°)$, and $A_p(90°, 0°)$. The following equation was used to calculate half the total shoot area:

$$A_s = 2\frac{\begin{array}{c}A_p(0°,0°)\cos(15°) + A_p(45°,0°)\cos(45°) \\ + A_p(90°,0°)\cos(75°)\end{array}}{\cos(15°) + \cos(45°) + \cos(75°)} \tag{10}$$

This is Eq. (4) simplified for three angle measurements. Chen (1996a) compared this simple three-angle method with 21- and 39-angle projection methods, the difference was within 2% in three stands and 5% in one stand, suggesting this simple three-angle method is accurate for our purpose.

4. Results

4.1. Needle-to-shoot area ratio

The values of the measured needle-to-shoot area ratio for five stands are summarized in Table 2. The mean value for the mature Douglas-fir stand is 1.66, in reasonable agreement with the value of 1.77 reported in Chen and Black (1992b) for the same species using only several shoot samples. The value of 1.61 for the young Douglas-fir stand is only slightly smaller than that for the mature stand. The mean values for a balsam fir stand in New Brunswick and a white pine stand in southern Ontario are 1.71 and 1.91, respectively. Both values are considerably larger than the mean value of 1.41 reported by Chen (1996a) for six black spruce (*Picea mariana* (Mill.) B.S.P.) and jack pine (*Pinus banksiana* Lamb.) stands in Saskatchewan and Manitoba. The value of 1.57 for a black spruce stand in Quebec is the intermediate case. It appears that the needle-to-shoot area ratio is mostly determined by the growth conditions. In areas with better growing conditions, needles in shoots are denser, making larger needle-to-shoot area ratios. The variations of this ratio among the nine classes of shoot samples show similar patterns as those found by Chen (1996a): (i) dominant trees generally have the largest values, followed by co-dominant and suppressed trees; (ii) shoots at higher levels generally have larger values. These systematic variation patterns and considerable differences among classes suggest that this shoot stratification strategy is necessary for obtaining a reliable mean value for a stand, and the accuracy can still increase if more shoot samples are analyzed.

Table 2
Needle-to-shoot area ratio (γ) of some of the coniferous species in Canada

	IDF	DF88	YBF	WPP39	EOBS
DT	2.00 ± 0.17	1.20 ± 0.04	2.29 ± 0.46	2.00 ± 0.24	1.70 ± 0.28
DM	1.67 ± 0.09	1.47 ± 0.14	1.73 ± 0.13	1.96 ± 0.14	1.51 ± 0.29
DL	1.15 ± 0.10	1.24 ± 0.07	1.40 ± 0.05	1.83 ± 0.26	1.28 ± 0.10
MT	1.66 ± 0.25	1.74 ± 0.12	1.83 ± 0.23	2.05 ± 0.16	1.60 ± 0.22
MM	1.59 ± 0.17	1.63 ± 0.12	1.85 ± 0.13	1.75 ± 0.23	1.64 ± 0.27
ML	1.65 ± 0.08	1.66 ± 0.52	1.34 ± 0.20	1.77 ± 0.14	1.66 ± 0.19
ST	1.61 ± 0.21	1.94 ± 0.09	1.87 ± 0.23	2.02 ± 0.20	1.67 ± 0.18
SM	1.57 ± 0.14	2.01 ± 0.26	1.65 ± 0.15	2.00 ± 0.11	–
SL	2.02 ± 0.12	1.57 ± 0.35	1.44 ± 0.05	1.85 ± 0.16	1.47 ± 0.13
Mean	1.66 ± 0.15	1.61 ± 0.19	1.71 ± 0.18	1.91 ± 0.18	1.57 ± 0.14

In each forest stand, 45 shoot samples were taken from three trees: one dominant (D), one co-dominant (M) and one suppressed (S), at three heights: top (T), middle (M) and bottom (L), forming nine classes with five shoot samples each: DT, DM, DL, MT, MM, ML, MS, ST, SM, and SL.

Table 3
Mean LAI values in forest sites in Fluxnet Canada Research Network, measured in 2003–2005

Site code	L_e LAI-2000		L_e TRAC	L_e DHP 55–60°	Green FPAR at noon 15 August	α	γ_E	Ω_E DHP 40–45°	Ω_E TRAC	LAI DHP	LAI TRAC	LAI TRAC + LAI-2000
	1–3[a]	1–5										
IDF	4.34	3.83	3.38	3.57	0.79	0.20	1.66	0.91	0.81	5.9	5.6	**7.3**
DF88	2.83	2.50	–	2.50	0.69	0.10	1.61	0.89	–	4.7	–	**4.7**[b]
OMW	3.90	3.53	–	3.69	0.78	0.15	1.15	0.93	–	4.5	–	**4.3**[b]
EOBS	2.65	2.11	2.22	1.68	0.62	0.15	1.57	0.88	0.92	3.0	3.3	**3.7**
BF80	6.47	5.37	5.65	4.35	0.87	0.15	1.71	0.95	0.96	7.7	8.5	**9.4**
IBF	6.28	5.11	5.75	4.90	0.86	0.20	1.71	0.95	0.96	8.2	8.7	**8.4**
YBF	6.24	5.13	5.19	5.07	0.86	0.20	1.71	0.96	0.94	8.4	7.5	**8.6**
WPP39	5.55	4.42	5.22	4.01	0.81	0.20	1.91	0.94	0.98	7.6	8.2	**8.0**
WP74	3.37	3.30	3.82	–	0.72	0.20	1.91	–	0.99	–	5.9	**5.9**
WPP89	7.11	6.77	6.23	–	0.91	0.15	1.91	–	1.0	–	10.2	**12.8**
F77	–	–	2.82	–	0.69	0.15	1.40	–	0.99	–	3.4	–
F98	–	–	1.31	–	0.34	0.40	1.40	–	0.97	–	1.1	–
OA	–	1.90	2.44	–	0.55	0.15	1.00	–	0.87	–	2.4	**2.1**
SOBS	–	2.57	2.72	–	0.65	0.15	1.36	–	0.90	–	3.5	**3.8**
SOJP	–	1.68	1.76	–	0.49	0.20	1.42	–	0.85	–	2.5	**2.6**
HJP75	–	1.86	2.07	–	0.54	0.15	1.44	–	0.93	–	3.1	**2.9**
HJP94	–	–	0.48	–	0.22	–	1.44	–	0.83	–	0.8	–

Also shown are all parameters needed to calculate LAI using Eq. (1). Three techniques are used: LAI-2000, TRAC and digital hemispherical photography (DHP). The combination of LAI-2000 and TRAC provides the best estimates (in **bold**). In the final LAI calculations, L_e values from LAI-2000 (rings 1–5) are increased by 16% to account for multiple scattering effect (see Section 4.2).

[a] Rings 4 and 5 in LAI-2000 data are blocked in processing.

[b] Ω_E from DHP is used in the absence of TRAC data.

4.2. Leaf area index

All parameters required for LAI estimation using Eq. (1) are summarized in Table 3. The final LAI values are given on three separate columns: (i) from the combination of TRAC (for clumping) and LAI-2000 (for L_e), which is in bold to indicate that this column gives the best estimates; (ii) from TRAC only; (iii) from DHP only. TRAC is capable of measuring both L_e and clumping, but in extensive stands, L_e measured at one or several zenith angles is less reliable as the stand average than that of LAI-2000 which is based on hemispherical measurements. However, the difference in LAI estimation with the added L_e information from LAI-2000 is found to be only mildly significant based on the comparison of the best estimates and the TRAC estimates (Fig. 1). Therefore, walking TRAC over a transect at a few zenith angles can generally obtain LAI values within 10% of the best estimate, and only in two cases, IDF and WP85, TRAC values are 23% and 26% smaller than the best estimates, respectively. At the IDF site, TRAC measurements were made in October 2005, while LAI-2000 measurements were made in August 2004, and the variations between years and between seasons might have contributed significantly to the differences between TRAC and the best estimate. At the WP85 site, the forest was very dense with little penetration of either direct or diffuse light, and the LAI measurements from all instruments were prone to error because the inverted LAI using the Beer's Law becomes highly sensitive to small errors in the radiation transmission measurements at high LAI values. However, there is little doubt that the LAI of the WP85 stand was larger than 10. For the OA site, the LAI is the mean of 3.1, 2.5, and 2.6 for 2003, 2004, and 2005, respectively, in the mid-summer for the overstorey only. The understorey LAI was generally as large as the overstorey, and the total LAI varied in the range from 3.7 to 5.2 in the period of 1994–2003 (Barr et al., 2004).

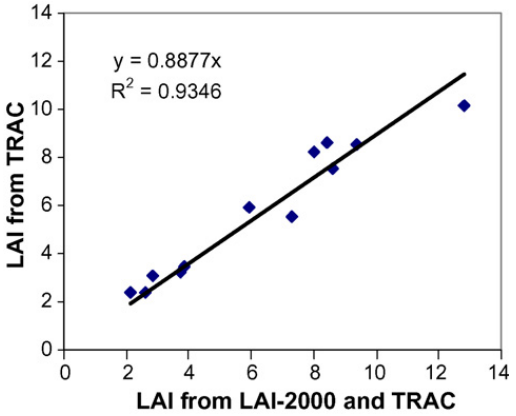

Fig. 1. Comparison of LAI values derived from TRAC with those derived from combining LAI-2000 for the effective LAI and TRAC for element clumping.

For most stands, LAI-2000 data were processed for L_e in two ways: (i) using all five rings, and (ii) using only rings 1–3, for the purpose of studying the multiple scattering effect (see Section 3.3 for reasons). It is interesting to note that L_e based on rings 1–3 is consistently larger than that based on rings 1–5, indicating indeed that stronger multiple scattering effects existed at larger zenith angles. The average difference between these two ways of L_e calculation is 16%. If the leaf angle distribution is spherical, the difference between these two cases in each stand can be entirely attributed to the multiple scattering effect. However, conifer canopies are complex with horizontal branches and vertical tree crowns, and the effective leaf angle distribution can deviate from the spherical distribution to a considerable extent. For Douglas-fir canopies with distinct horizontal branches, causing the extinction coefficient to decrease with zenith angle (Chen and Black, 1991), the L_e measured in near the vertical direction is larger than that in near the horizontal direction, and the difference in L_e between these two angle ranges (1–3 and 1–5 rings) may be partly offset by this structural effect, i.e. the difference is smaller than the scattering effect alone. For black spruce, where the vertical crown structures are more apparent than the short horizontal branches, making the extinction coefficient increase with zenith angle (Chen, 1996b), the difference may be larger than the multiple scattering effect alone. In terms of angular canopy structure, balsam fir and eastern white pine may be the intermediate cases between Douglas-fir and black spruce. As these angular structural effects on the difference in L_e estimated in the two zenith angle ranges differ in different stands, some positive and some negative, we estimate the multiple scattering effect by simply taking the arithmetic mean of the ratio of the L_e value calculated in rings 1–3 to that calculated in rings 1–5, with the assumption that structural effects average out in stands of contrasting angular structures. The average ratio is 1.16, meaning that the multiple scattering effect caused a negative bias of 16% in L_e in these stands. We have therefore increased all L_e values from LAI-2000 and DHP (except those from TRAC) by 16% in the final calculation of LAI (the listed L_e values are not corrected using this ratio).

If TRAC could be used to obtain the same spatial and angular averages as the LAI-2000, it would be the ultimate way to find this light scattering effect on L_e, but in reality this is difficult to achieve because TRAC only measures in sun's azimuthal direction. In Table 3, the L_e values from TRAC are generally larger than those from LAI-2000 including five rings, also indicating the same light scattering effect. However, in two stands (IDF and WP85), the TRAC values are even smaller than LAI-2000 values for reasons given in the first paragraph of this section. Through comparing L_e from TRAC measurements made at 5–13 zenith angles with those from LAI-2000 based on rings 1–5, Chen (1996b) found that the multiple scattering effect was in the range from 0% to 25% for six conifer stands with a mean of 15%, in good agreement with the value of 16% found in this study through LAI-2000 ring masking.

The woody-to-total area ratio (α) is estimated based on visual examination of woody (stem and branch) areas appearing in photographs and previous values measured or estimated by Chen (1996a) for stands in Saskatchewan. For the OA site, it was obtained through LAI-2000 measurements before the growing season (Barr et al., 2004). For conifer sites, these estimates may be most uncertain among all parameters in Table 3. At the F98 site where many dead trees are still standing after the fire in 1998, the α value is estimated to be 40%. The needle-to-shoot area ratio (γ) is mostly based on new measurements made in this study. For stands in Saskatchewan, values previously measured by Chen (1996a) are used. For the mixed wood stand near Timmins, the value of 1.15 was derived as the weighted average between broadleaf trees ($\gamma = 1.0$) and conifer trees ($\gamma = 1.57$, taken as the value of EOBS stand in Quebec). The weights between these two types of trees were obtained through basal area measurements using a prism along the transect.

The accuracy of the best estimates of LAI is conservatively estimated to be 75%, or the total error is 25%, including 10% error in woody-to-total area ratio, 5% error in effective LAI, 5% in needle-to-shoot error ratio, and 5% in element clumping index. In black spruce stands, where the top portion of tree crowns is very dense, there could be an additional 10% underestimation of LAI (Chen et al., 1997).

4.3. Reliability of digital hemispherical photography (DHP)

The reliability of the DHP technique may be examined in two ways: (i) its ability to acquire reliable L_e values, and (ii) its ability to measure the element clumping index. First, we carried out point-by-point comparison of L_e measurements by both DHP and LAI-2000 for all available points from all sites (Fig. 2). In field measurements, we took LAI-2000 data every 10 m, while photographs were generally taken every 50 m because it was more time consuming. It is encouraging to see that overall DHP agreed very well with LAI-2000 in terms of L_e. As the stand average, the largest difference is 21% at the EOBS site (Table 3). The agreement could

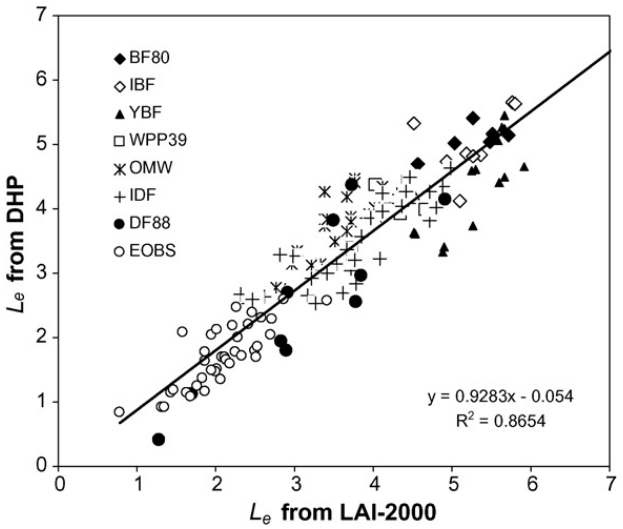

Fig. 2. Comparison of effective LAI (L_e) values measured using the digital hemispherical photography (DHP) technique with those measured using LAI-2000.

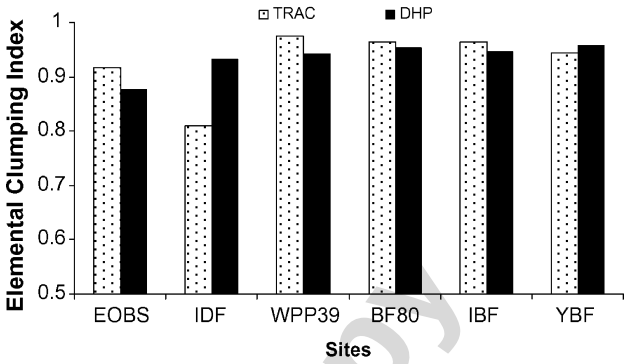

Fig. 3. Comparison of the element clumping index measured using the digital hemispherical photography (DHP) technique with those measured using TRAC.

have been better if the angular exposure and the spatial positions of these two sensors at each flag position were exactly same, but in practice, a 90° view cap was used for LAI-2000 while photographs were exposed to all azimuthal directions, and for the convenience of operation, the DHP camera was normally mounted at 1 m above the ground while LAI-2000 was put at about 0.5 m above the ground. This good agreement between these two techniques is found because (i) LAI-2000 was reliable when operated properly (see Section 3.3) and (ii) strict procedures were followed for DHP exposure setting and image processing (see Section 3.4). We emphasize that the DHP exposure setting is critical for correct determination of L_e. If the automatic exposure inside the stand was used (as done in many other studies), the L_e from DHP would have been underestimated by over 40% in comparison with LAI-2000 (Zhang et al., 2005). The automatic exposure causes this underestimation because it overexposes the canopy to obtain the mean grey level of 18% while our purpose is to make the canopy black and sky white. The correct exposure is two-stops over-exposure relative to the automatic sky exposure determined outside the stand in order to make sky appear white. The automatic exposure determined inside the stand is normally one to four stops more exposure (either longer time or larger aperture) than the correct exposure depending on the LAI of the stand. In denser stands, the difference in these two exposure settings is larger, causing larger underestimation in L_e.

The element clumping index determined from DHP compared reasonably well with TRAC measurements (Fig. 3). We averaged the clumping index values from all correctly exposed photographs taken in each stand to compare with the mean value from TRAC, in order to minimize the problem of different samplings of these techniques (TRAC samples a straight line in space, while DHP samples a circle in the canopy). Overall, DHP obtains values of the clumping index within 4% of the TRAC value with the exception at the IDF site, where the DHP value is larger than the TRAC value by 12%. This again could have been caused by the different dates of measurements of these two sensors. TRAC was used a year later than DHP and near the end of the growing season, and there could be some differences in the canopy between these 2 years and between seasons. We do not find this comparison of these two techniques to be assertive in terms of DHP's ability to determine clumping. Visual examination of DHP photographs does reveal much detailed canopy structural information, and clumping can indeed be derived from DHP. However, two nontrivial technical issues still remain: (i) because of the multiple scattering effect, a significant fraction of leaves near the vertical direction are lost even the exposure is correctly determined, and this is balanced by underexposing the canopy in near the horizontal direction (to get correct L_e), causing losses of small gaps at large zenith angles. So a compromise of using the zenith angles of 40–45° in determining the clumping value was made in this study; (ii) because of the loss of small gaps, the gap size distribution is distorted, and this distortion increases with zenith angle. We used the method of Chen and Black (1992b) to determine the projected element width from the gap size distribution curve (tangent of the log curve at zero gap size) and found that the width determined in this way was much larger than the characteristic width of shoots in the canopy (up to 10 times) and was increasing with zenith angle, suggesting that as the zenith angle increased, the ability of DHP to differentiate shoots

decreased. These two issues may be inherent problems with the DHP technique, and we therefore suggest that we are not yet ready to replace existing optical instruments with DHP for LAI measurements, especially when high accuracy is required. However, DHP techniques can be used for fast and reasonably accurate (75–85%) measurements of LAI by determining the correct exposure in the field and by selecting correct zenith angle ranges in photograph processing: 55–60° for L_e and 40–45° for clumping.

4.4. Fraction of photosynthetically active radiation (FPAR) absorbed by the canopy

FPAR is a parameter needed in light use efficiency models, although these models suffer from serious inaccuracy in photosynthesis estimation because of their inability to differentiate diffuse and direct light effects (Chen et al., 2003). FPAR was measured accurately using TRAC because the technique of walking and high frequency sampling of the transmitted and reflected PAR is the most reliable way to obtain the spatial averages of these PAR components in forest canopies, but the measurements were made in a limited number of sun angles in each stand. However, we should note that FPAR is not an inherent canopy parameter. For the same canopy, FPAR changes greatly with solar zenith angle, and therefore it is diurnally and seasonally variable. For convenience of potential users, we provide FAPR values at the solar noon of 15 August for all stands in Table 3. They are calculated using the unmasked LAI-2000 L_e data in Table 3 (after making the 16% correction, see Section 4.2). L_e from LAI-2000 rather than from TRAC is used for FPAR estimation because LAI-2000 provides better spatial and angular averages than TRAC. For conifer stands, L_e is almost constant throughout the year (Chen, 1996b), and it can be used to calculate FPAR for any given time on the day and in any season. The following equation (Chen, 1996b) can be used for this purpose:

$$\mathrm{FPAR} = (1 - \rho_a) - (1 - \rho_u)\, e^{-0.45(1-\alpha)L_e/\cos\theta} \qquad (11)$$

where ρ_a is the PAR albedo above the canopy, and ρ_u is the PAR albedo of the forest floor. They were found to be 0.05 and 0.06 for conifer stands, respectively (Chen, 1996b). For simplicity, a constant of 0.45 is given as the extinction coefficient for the global PAR in consideration of the multiple scattering effect on enhancing the PAR transmission, and the L_e values in Table 3 should be multiplied by a factor 1.16 before using Eq. (11). The woody fraction (α) is discounted from L_e in order to obtain FPAR for green leaves only. Given the L_e value, it is critical to know the solar zenith angle θ. As θ is larger in winter than in summer, the FPAR is also larger in winter (counter intuitive).

5. Conclusions

Through a large team effort, we report LAI values and their components for all major forest sites in Fluxnet Canada Research Network. The accuracy of the final LAI values is estimated to be generally higher than 75% except for black spruce stands which may have an additional 10% underestimation because of extremely dense crown tops. The largest improvements made in this study are the systematic and labour-intensive laboratory measurements of the needle-to-shoot area ratio for five conifer stands. This ratio quantifies a level of foliage clumping that could not be measured in the field. The largest uncertainty in the reported LAI values exists in the estimation of the effect of non-green materials on the indirect measurements of the green leaf area index. This may be a direction to improve in the near future.

Three instruments are compared, including LAI-2000, TRAC and digital hemispherical photography (DHP). Measurements are the best made with the combined use of LAI-2000 for the effective LAI based on hemispherical diffuse radiation transmission and TRAC for the element clumping index based on direct radiation transmission. The DHP technique is shown here to be capable of obtaining similar (within 25% maximum) measurements as those from combining LAI-2000 and TRAC, when the DHP was used following strict procedures of photograph exposure and processing. However, LAI-2000 and TRAC are still considered to be more reliable than DHP because of some remaining inherent technical issues with the DHP technique. These issues may add an error of up to 25% in addition to LAI-2000 and TRAC errors.

Acknowledgements

This work was supported by the Fluxnet Canada Research Network funded by the Natural Science and Engineering Council of Canada, the Canadian Foundation of Climate and Atmospheric Sciences, and BIOCAP Canada. Gang Mo of University of Toronto assisted in part of the field measurements. We gratefully acknowledge the logistic support from various people during the field experiments: Zhisheng Xing, Charles Bourque, and Edwin Swift at the New Brunswick sites; Andre Beaudoin, Luc Guindon and Pierre Bernier for

the Chibogamou site in Quebec; Harry McCaughey at the Timmins site in Ontario; Altaf Arain at the Turkey Lake sites in Ontario; and Andy Black at the Campbell River sites in B.C. Alison Sass and Natasha Neumann provided assistance in LAI measurements in the various sites in Saskatchewan. Nick Grant did TRAC measurements at one of the Campbell River sites.

References

Anderson, M.C., 1964. Studies of woodland light climate. Part 1. The photographic computation of light conditions. J. Ecol. 52, 27–41.

Baret, F., Andrieu, B., Folmer, J.C., Hanocq, J.F., Sarrouy, C., 1993. Gap fraction measurement using hemispherical infrared photographies and its use to evaluate PAR interception efficiency. In: Varlet-Grancher, C., Bonhomme, R., Sinoquet, H. (Eds.), Crop Structure and Light Microclimate: Characterization and Applications. INRA, Paris, pp. 359–372.

Barr, A.G., Black, T.A., Hogg, E.H., Kljun, N., Morgenstern, K., Nesic, Z., 2004. Inter-annual variability of leaf area index of boreal aspen-hazelnut forest in relation to net ecosystem production. Agric. For. Meteorol. 126, 237–255.

Brown, H.E., 1962. The canopy camera. US For. Ser. Rocky Mount For. Ecol. Manage. 11, 139–144.

Chan, S.S., McCreight, R.W., Walslad, J.D., Spies, T.A., 1986. Evaluating forest cover with computerized analysis of fisheye photographs. For. Sci. 32, 1085–1091.

Chen, J.M., 1996a. Optically-based methods for measuring seasonal variation in leaf area index of boreal conifer forests. Agric. For. Meteorol. 80, 135–163.

Chen, J.M., 1996b. Canopy architecture and remote sensing of the fraction of photosynthetically active ration absorbed by boreal conifer forests. IEEE Trans. Geosci. Remote Sens. 34, 1353–1368.

Chen, J.M., Black, T.A., 1991. Measuring leaf area index of plant canopies with branch architecture. Agric. For. Meteorol. 57, 1–12.

Chen, J.M., Black, T.A., 1992a. Defining leaf area index for non-flat leaves. Plant Cell Environ. 15, 421–429.

Chen, J.M., Black, T.A., 1992b. Foliage area and architecture of clumped plant canopies from sunfleck size distributions. Agric. For. Meteorol. 60, 249–266.

Chen, J.M., Black, T.A., Adams, R.S., 1991. Evaluation of hemispherical photography for determining plant area index and geometry of a forest stand. Agric. For. Meteorol. 56, 129–143.

Chen, J.M., Cihlar, J., 1995. Plant canopy gap-size analysis theory for improving optical measurements of leaf area index. Appl. Opt. 34 (27), 6211–6222.

Chen, J.M., Rich, P.M., Gower, S.T., Norman, J.M., Plummer, S., 1997. Leaf area index of boreal forests: theory, techniques, and measurements. J. Geophys. Res. 102 (D24), 29429–29443.

Chen, J.M., Pavlic, G., Brown, L., Cihlar, J., Leblanc, S.G., White, H.P., Hall, R.J., Peddle, D., King, D.J., Trofymow, J.A., Swift, E., Van der Sanden, J., Pellikka, P., 2002. Derivation and validation of Canada-wide coarse resolution leaf area index maps using high-resolution satellite imagery and ground measurements. Remote Sens. Environ. 80, 165–184.

Chen, J.M., Liu, L., Leblanc, S.G., Lacaze, R., Roujean, J.L., 2003. Multi-angular optical remote sensing for assessing vegetation structure and carbon absorption. Remote Sens. Environ. 84, 516–525.

Coursolle, C., Margolis, H.A., Barr, A.G., Black, T.A., Amiro, B.D., McCaughey, J.H., Flanagan, L.B., Lafleur, P.M., Roulet, N.T., Bourque, C.P.-A., Arain, M.A., Wofsy, S.C., Dunn, A., Morgenstern, K., Orchansky, A.L., Bernier, P.Y., Chen, J.M., Kidston, J., Saigusa, N., Hedstrom, N., 2006. Late-summer carbon fluxes from Canadian forests and peatlands along an east-west continental transect. Can. J. For. Res. 36, 783–800.

Englund, S.R., O'Brien, J.J., Clark, D.B., 2000. Evaluation of digital and film hemispherical photography and spherical densiometry for measuring forest light environments. Can. J. For. Res. 30, 1999–2005.

Fassnacht, K., Gower, S.T., Norman, J.M., McMurtrie, R.E., 1994. A comparison of optical and direct methods for estimating foliage surface area index in forests. Agric. For. Meteorol. 71, 183–207.

Frazer, G.W., Fournier, R.A., Trofymow, J.A., Hall, J.R., 2001. A comparison of digital and film fisheye photography for analysis of forest canopy structure and gap light transmission. Agric. For. Meteorol. 109, 249–263.

Gower, S.T., Norman, J.M., 1990. Rapid estimation of leaf area index in forests using the LI-COR LAI-2000. Ecology 72, 1896–1900.

Gower, S.T., Kucharik, C.J., Norman, J.M., 1999. Direct and indirect estimation of leaf area index, fAPAR, and net primary production of terrestrial ecosystems. Remote Sens. Environ. 70, 29–51.

Jonckheere, I., Fleck, S., Nackaerts, K., Muys, B., Coppin, P., Weiss, M., Baret, F., 2004. Methods for leaf area index determination. Part I. Theories, techniques and instruments. Agric. For. Meteorol. 121, 19–35.

Kucharik, C.J., Norman, J.M., Murdock, L.M., Gower, S.T., 1997. Characterizing canopy non-randomness with a multiband vegetation imager (MVI). J. Geophys. Res. 102 (D24), 29455–29473.

Kucharik, C.J., Norman, J.M., Gower, S.T., 1998. Measurements of brach area and adjusting leaf area index indirect measurements. Agric. For. Meteorol. 91, 69–88.

Kucharik, C.J., Norman, J.M., Gower, S.T., 1999. Characterization of radiation regimes in nonrandom forest canopies: theory, measurements, and a simplified modeling approach. Tree Physiol. 19, 695–706.

Leblanc, S.G., 2002. Correction to the plant canopy gap size analysis theory used by the tracing radiation and architecture of canopies (TRAC) instrument. Appl. Opt. 31 (36), 7667–7670.

Leblanc, S.G., Chen, J.M., Fernandes, R., Deering, D.W., Conley, A., 2005. Methodology comparison for canopy structure parameters extraction from digital hemispherical photography in boreal forests. Agric. For. Meteorol. 129, 187–207.

Miller, J.B., 1967. A formula for average foliage density. Aust. J. Bot. 15, 141–144.

Nilson, T., 1971. A theoretical analysis of the frequency of gaps in plant stands. Agric. Meteorol. 8, 25–38.

Olsson, L., Carlsson, K., Grip, H., Perttu, K., 1982. Evaluation of forest-canopy photographs with diode-array scanner OSIRIS. Can. J. For. Res. 12, 822–828.

Oker-Blom, P., 1986. Photosynthetic radiation regime and canopy structure in modeled forest stands. Acta For. Fenn. 197, 1–44.

Peichl, M., Arain, M.A., 2006. Above- and belowground ecosystem biomass and carbon pools in an age-sequence of planted white pine forests. Agric. For. Meteorol. 140, 51–63.

Rich, P., 1990. Characterising plant canopies with hemispherical photographs. Remote Sens. Rev. 5 (1), 13–29.

Stenberg, P., Linder, S., Smolander, H., Flower-Ellis, J., 1994. Performance of the LAI-2000 plant canopy analyzer in estimating leaf area index of some Scots pine stands. Tree Physiol. 14, 981–995.

Wagner, S., 2001. Relative radiance measurements and zenith angle dependent segmentation in hemispherical photography. Agric. For. Meteorol. 107, 103–115.

Walter, J.-M., Fournier, R.A., Soudani, K., Meyer, E., 2003. Integrating clumping effects in forest canopy structure: an assessment through hemispherical photographs. Can. J. Remote Sens. 29 (3), 388–410.

Weiss, M., Baret, F., Smith, G.J., Jonckheere, I., Coppin, P., 2004. Review of methods for in situ leaf area index (LAI) determination. Part II. Estimation of LAI, errors and sampling. Agric. For. Meteorol. 121, 37–53.

Whitford, K.R., Colquhoun, I.J., Lang, A.R.G., Harper, B.M., 1995. Measuring leaf area index in a sparse eucalypt forest: a comparison of estimate from direct measurement, hemispherical photography, sunlight transmittance, and allometric regression. Agric. For. Meteorol. 74, 237–249.

Zhang, Y., Chen, J.M., Miller, J., 2005. Determining exposure of digital hemispherical photographs for leaf area index estimation. Agric. For. Meteorol. 133, 166–181.